

Nonlinear optics and spontaneous parametric down-conversion

Down-conversion results from a nonlinear interaction of pump radiation with media where the induced polarization is so strongly effected by the radiation that it deforms beyond the linear response that generates the usual dispersion and absorption. For our purposes, we can expand the nonlinear polarization in a power series in the applied radiation field. Crystals commonly used in nonlinear optics are highly anisotropic and their response is described in tensorial form according to

$$\hat{P}_i = \chi_{i,j}^{(1)} \hat{E}_j + \chi_{i,j,k}^{(2)} \hat{E}_j \hat{E}_k + \chi_{i,j,k,l}^{(3)} \hat{E}_j \hat{E}_k \hat{E}_l + \dots \quad (\text{D1})$$

where $\chi^{(m)}$ is the m th-order electric susceptibility tensor [1] and where repeated indices imply a sum. The energy density is then $\varepsilon_0 E_i P_i$ and thus the *second-order* contribution to the Hamiltonian, the interaction Hamiltonian, is

$$\hat{H}^{(2)} = \varepsilon_0 \int_V d^3 \mathbf{r} \chi_{i,j,k}^{(2)} \hat{E}_i \hat{E}_j \hat{E}_k, \quad (\text{D2})$$

where the integral is over the interaction volume. We now represent the compo-

where the integral is over the interaction volume. We now represent the components of the fields as Fourier integrals of the form

$$\hat{E}(\mathbf{r}, t) = \int d^3\mathbf{k} \left[\hat{E}^{(-)}(\mathbf{k}) e^{-i[\omega(\mathbf{k})t - \mathbf{k}\cdot\mathbf{r}]} + \hat{E}^{(+)}(\mathbf{k}) e^{i[\omega(\mathbf{k})t - \mathbf{k}\cdot\mathbf{r}]} \right], \quad (\text{D3})$$

where

$$\hat{E}^{(-)}(\mathbf{k}) = i\sqrt{\frac{2\pi\hbar\omega(\mathbf{k})}{V}} \hat{a}^\dagger(\mathbf{k}), \text{ and } \hat{E}^{(+)}(\mathbf{k}) = i\sqrt{\frac{2\pi\hbar\omega(\mathbf{k})}{V}} \hat{a}(\mathbf{k}). \quad (\text{D4})$$

The operators $\hat{a}(\mathbf{k})$ and $\hat{a}^\dagger(\mathbf{k})$ are the annihilation and creation operators respectively of photons with momentum $\hbar\mathbf{k}$.* If we substitute field expressions of the above form into Eq. (D2) and retain only the terms important for the case when the signal and idler modes are initially in vacuum states, we obtain the interaction Hamiltonian

$$\begin{aligned} \hat{H}_I(t) = & \varepsilon_0 \int_V d^3\mathbf{r} \int d^3\mathbf{k}_s d^3\mathbf{k}_i \chi_{lmn}^{(2)} \\ & \times \hat{E}_{\text{pl}}^{(+)} e^{i[\omega_p(\mathbf{k}_p)t - \mathbf{k}_p \cdot \mathbf{r}]} \hat{E}_{\text{sm}}^{(-)} e^{-i[\omega_s(\mathbf{k}_s)t - \mathbf{k}_s \cdot \mathbf{r}]} \hat{E}_{\text{in}}^{(-)} e^{-i[\omega_i(\mathbf{k}_i)t - \mathbf{k}_i \cdot \mathbf{r}]} + H.c. \end{aligned} \quad (\text{D5})$$

The conversion rates for the process depend on the second order electric susceptibility $\chi^{(2)}$ but typically have efficiencies in the range 10^{-7} to 10^{-11} , extremely low rates. For this reason, in order to obtain significant output in the signal and idler beams it is necessary to pump the medium with a very strong coherent field which we can model as a classical field obtained from a laser as long as we are interested in interactions over a short enough time such that depletion of pump photons can be ignored – the parametric approximation. The pump laser is usually in the ultraviolet while the photons arising from the down-conversion are usually in the visible spectral range.

From time dependent perturbation theory, assuming the initial states of the signal and idler modes are in vacuum states, which we denote for the moment as $|\Psi_0\rangle$, we obtain, to first order, $|\Psi\rangle \approx |\Psi_0\rangle + |\Psi_1\rangle$ where [2]

$$\begin{aligned} |\Psi_1\rangle &= -\frac{i}{\hbar} \int dt \hat{H}(t) |\Psi_0\rangle \\ &= \mathcal{N} \int d^3\mathbf{k}_s d^3\mathbf{k}_i \delta(\omega_p - \omega_s(\mathbf{k}_s) - \omega_i(\mathbf{k}_i)) \\ &\quad \times \delta^{(3)}(\mathbf{k}_p - \mathbf{k}_s - \mathbf{k}_i) \hat{a}_s^\dagger(\mathbf{k}_s) \hat{a}_i^\dagger(\mathbf{k}_i) |\Psi_0\rangle, \end{aligned} \quad (\text{D6})$$

where \mathcal{N} is a normalization factor into which all constants have been absorbed.

One sees that the delta functions contain the phase matching conditions

$$\begin{aligned}\omega_p &= \omega_s + \omega_i, \\ \mathbf{k}_p &= \mathbf{k}_s + \mathbf{k}_i.\end{aligned}\tag{D7}$$

There are, in fact, two types of SPDC process. In type I, the signal and idler photons have the same polarization but these are orthogonal to that of the pump.

In the case of type I phase matching, we end up with the state given by Eq. (9.9), which we arrived at by assuming specific momenta which can be post-selected by the placement of a screen with properly located holes over the output of the down-converter.

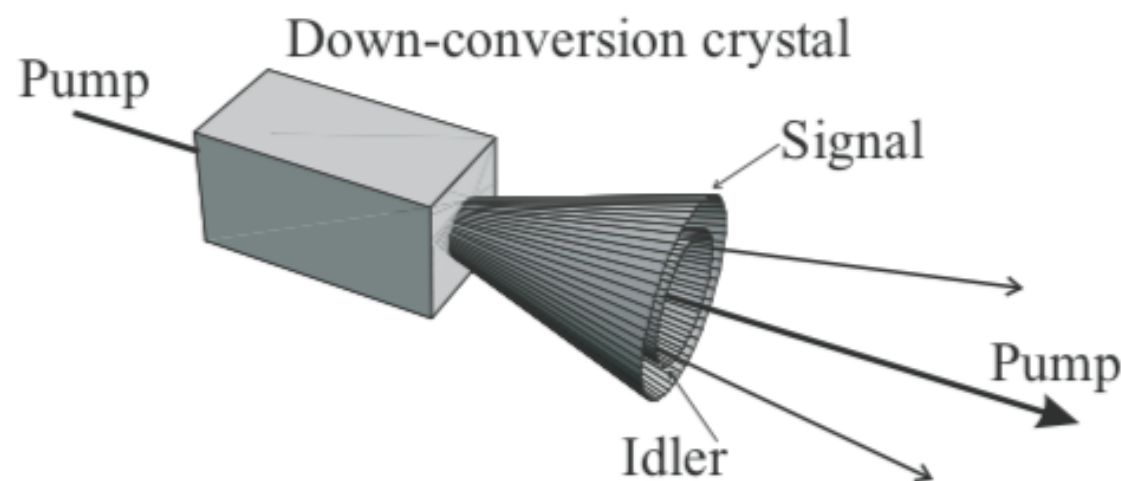
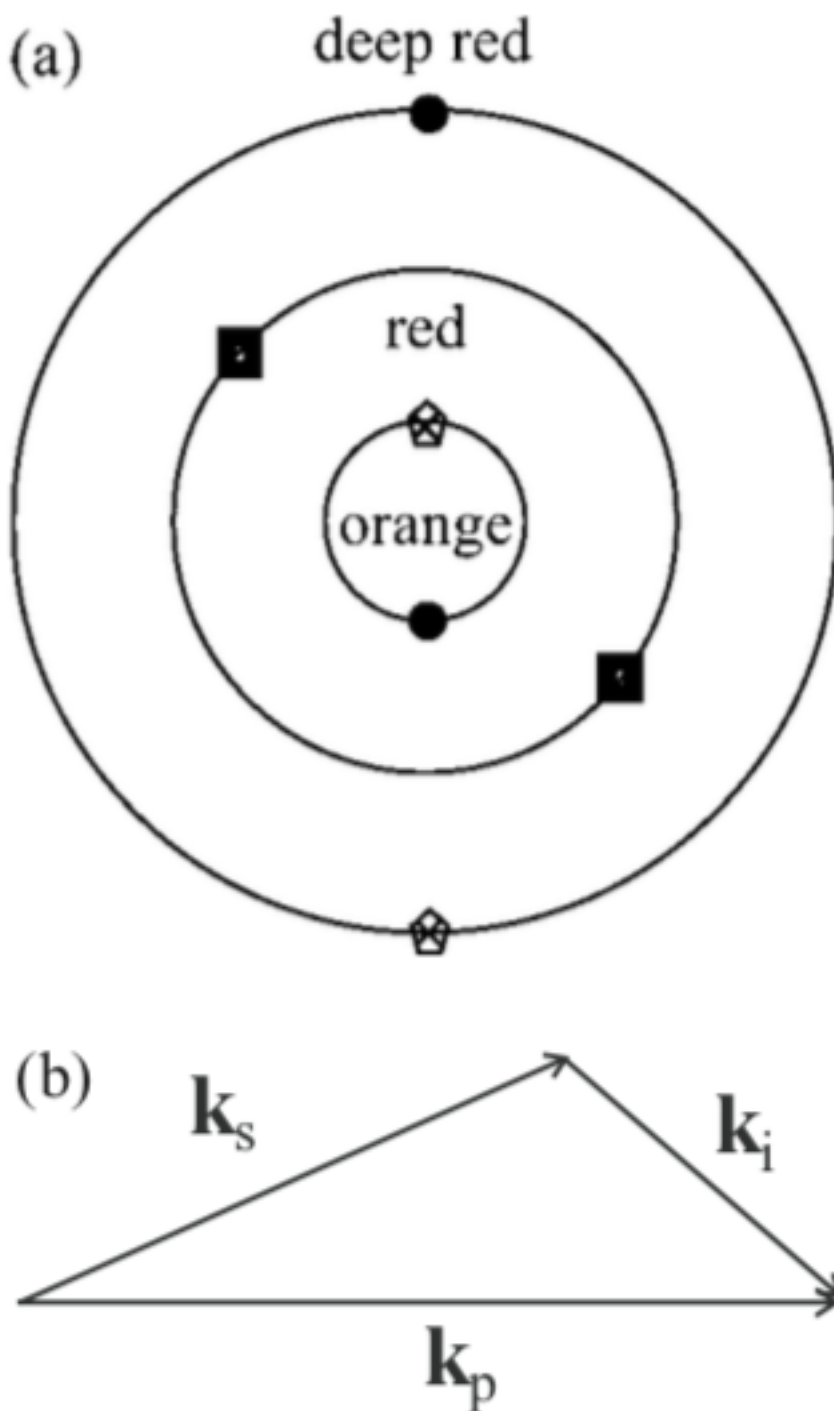


Fig. 9.1. Type I down-conversion. Photons from the pump beam are converted into signal and idler photons that emerge from the crystal along different directions. The signal and idler photons have identical polarization but orthogonal to that of the pump. The possible directions form a set of concentric cones. The light from the different cones is of different colors, typically orange near the center to a deep red at wider angles. The pump beam is in the ultraviolet.

Fig. 9.2. (a) A cross-section of the cones of light emerging from a type I down-converter. Like symbols represent conjugate photons satisfying the phase-matching condition. Note that those on the middle circle are degenerate in frequency. (b) A graphical view of the phase-matching condition.



In type II down-conversion, the signal and idler photons have orthogonal polarizations. Because of birefringence effects, the generated photons are emitted along two cones, one for the ordinary (o) wave and another for the extraordinary (e) wave, as indicated in Fig. 9.3. The intersection of the cones provides a means for generating polarization-entangled states. We use the notation $|V\rangle$ and $|H\rangle$ to represent vertically and horizontally polarized *single-photon* states. For photons that emerge along the intersections of the cones, with photons from other parts of the cones being excluded by screens with pinholes in front of the intersection points, there will be an ambiguity as to whether the signal or idler photons will be vertically or horizontally polarized, as indicated in Fig. 9.4. The Hamiltonian describing this is given by

$$\hat{H}_I = \hbar\eta\left(\hat{a}_{Vs}^\dagger\hat{a}_{Hi}^\dagger + \hat{a}_{Hs}^\dagger\hat{a}_{Vi}^\dagger\right) + H.c., \quad (9.6)$$

where the operators \hat{a}_{Vs}^\dagger , \hat{a}_{Hs}^\dagger , \hat{a}_{Vi}^\dagger , and \hat{a}_{Hi}^\dagger are the creation operators for photons with vertical and horizontal polarization for the signal and idler beams, respectively. Again, this Hamiltonian represents the post-selection obtained by placing a screen in front of the source with pinholes located just in the regions of the overlapping beams.

Fig. 9.3. Type II down-conversion. The signal and idler photons have orthogonal polarizations. Birefringence effects cause the photons to be emitted along two intersecting cones, one of the ordinary (*o*) ray and the extraordinary (*e*) ray.

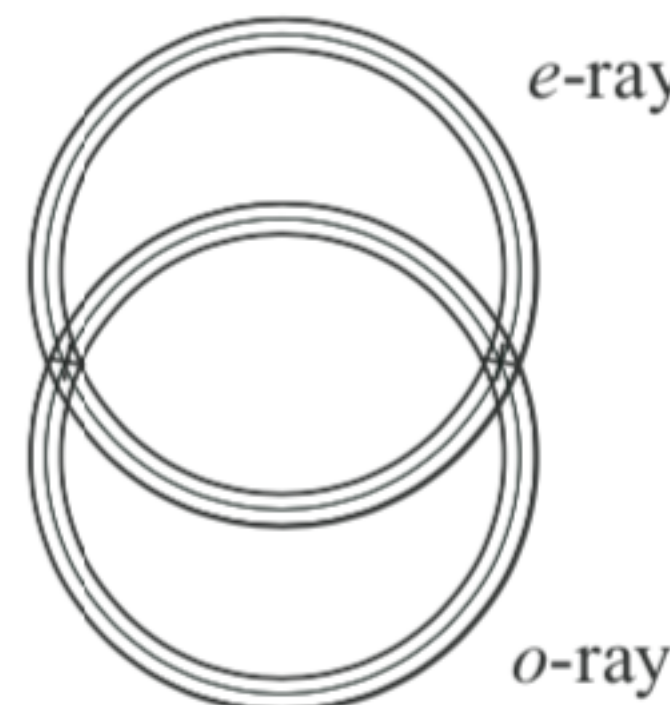
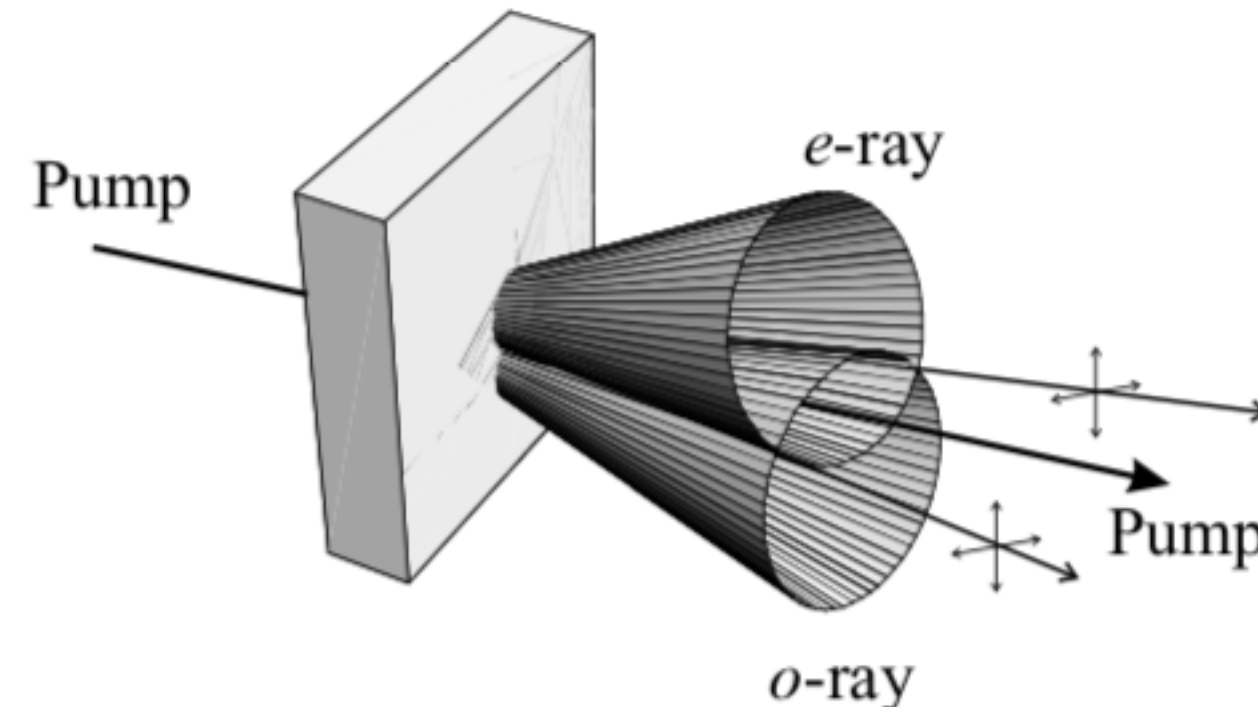
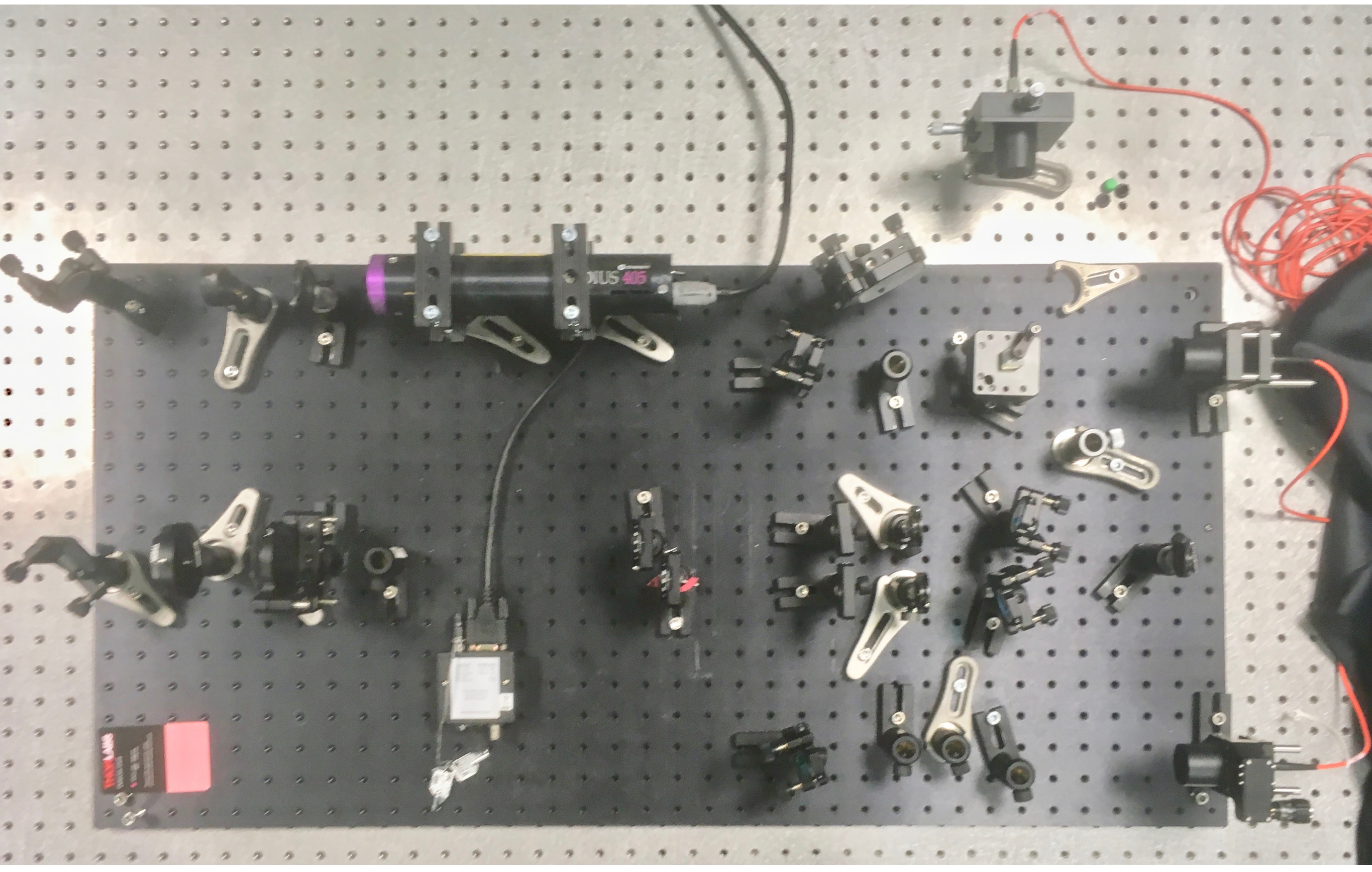


Fig. 9.4. The intersections of the cones for the *o*-ray and the *e*-ray are the sources for polarization entangled light. From these points it is not possible to tell from which beam a photon is obtained. The Hamiltonian in Eq. (9.6) describes the light taken from both intersections.



Let us take the initial state of the signal and idler modes to be represented by $|\Psi_0\rangle = |\{0\}\rangle$, which is the collective vacuum state for either type I or type II down-conversion. In either case, the state vector evolves according to

$$|\Psi(t)\rangle = \exp(-it\hat{H}_I/\hbar)|\Psi_0\rangle, \quad (9.7)$$

which we expand, since \hat{H}_I has no explicit time dependence, as

$$|\Psi(t)\rangle \approx [1 - it\hat{H}_I/\hbar + \frac{1}{2}(-it\hat{H}_I/\hbar)^2]|\Psi_0\rangle \quad (9.8)$$

to second order in time. If we consider the type I SPDC then $|\Psi_0\rangle = |0\rangle_s|0\rangle_i$ and we have

$$|\Psi(t)\rangle = (1 - \mu^2/2)|0\rangle_s|0\rangle_i - i\mu|1\rangle_s|1\rangle_i \quad (9.9)$$

where $\mu = \eta t$. This state vector is normalized to first order in μ and we have dropped the term of order μ^2 containing the state $|2\rangle_s|2\rangle_i$. In the case of type II SPDC with the initial state $|\Psi_0\rangle = |0\rangle_{Vs}|0\rangle_{Hs}|0\rangle_{Vi}|0\rangle_{Hi}$, we have

$$\begin{aligned} |\Psi(t)\rangle &= (1 - \mu^2/2)|0\rangle_{Vs}|0\rangle_{Hs}|0\rangle_{Vi}|0\rangle_{Hi} \\ &\quad - i\mu\frac{1}{\sqrt{2}}(|1\rangle_{Vs}|0\rangle_{Hs}|0\rangle_{Vi}|1\rangle_{Hi} + |0\rangle_{Vs}|1\rangle_{Hs}|1\rangle_{Vi}|0\rangle_{Hi}). \end{aligned} \quad (9.10)$$

We now define the vertically and horizontally polarized vacuum and single photon states as $|0\rangle := |0\rangle_V|0\rangle_H$, $|V\rangle := |1\rangle_V|0\rangle_H$, and $|H\rangle := |0\rangle_V|1\rangle_H$, so that we may write

$$|\Psi(t)\rangle = (1 - \mu^2/2)|0\rangle_s|0\rangle_i - i\mu(|V\rangle_s|H\rangle_i + |H\rangle_s|V\rangle_i). \quad (9.11)$$

The state in the second term, which when normalized reads

$$|\Psi^+\rangle = \frac{1}{\sqrt{2}}(|V\rangle_s|H\rangle_i + |H\rangle_s|V\rangle_i), \quad (9.12)$$

is one member out of a set of four states known as Bell states. The full set of Bell states is

$$|\Psi^\pm\rangle = \frac{1}{\sqrt{2}}(|H\rangle_1|V\rangle_2 \pm |V\rangle_1|H\rangle_2), \quad (9.13)$$

$$|\Phi^\pm\rangle = \frac{1}{\sqrt{2}}(|H\rangle_1|H\rangle_2 \pm |V\rangle_1|V\rangle_2). \quad (9.14)$$

We shall discuss these states, and their implications, in Section 9.6.

A.2 Two-state system and the Bloch sphere

For a two-state system, be it a spin- $1/2$ particle, a two-level atom, or the polarizations of a single photon, there always exists a description in terms of the Pauli operators $\hat{\sigma}_1$, $\hat{\sigma}_2$, $\hat{\sigma}_3$ satisfying the commutation relations

$$[\hat{\sigma}_i, \hat{\sigma}_j] = 2i\varepsilon_{ijk}\hat{\sigma}_k. \quad (\text{A23})$$

In a basis where $\hat{\sigma}_3$ and $\hat{\sigma}^2 = \hat{\sigma}_1^2 + \hat{\sigma}_2^2 + \hat{\sigma}_3^2$ are diagonal, these operators can be written in matrix form as

$$\sigma_1 = \begin{pmatrix} 0 & 1 \\ 1 & 0 \end{pmatrix}, \quad \sigma_2 = \begin{pmatrix} 0 & -i \\ i & 0 \end{pmatrix}, \quad \sigma_3 = \begin{pmatrix} 1 & 0 \\ 0 & -1 \end{pmatrix}. \quad (\text{A24})$$

Any Hermitian 2×2 matrix can be expressed in terms of the Pauli matrices and the 2×2 identity matrix \hat{I}_2 , and this includes, of course, the density operator.

— .

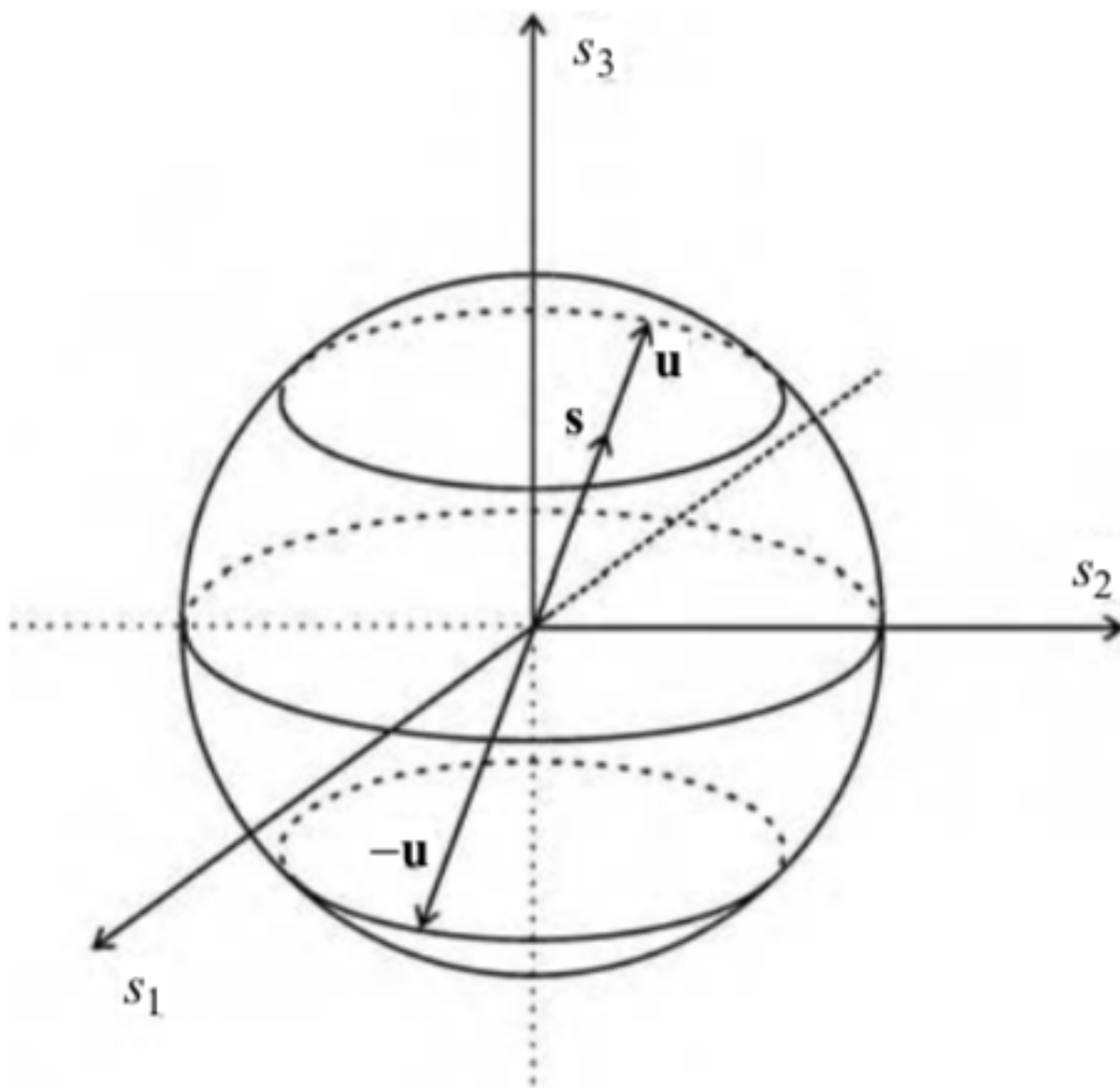
That is, we can write

$$\rho = \begin{pmatrix} \rho_{11} & \rho_{12} \\ \rho_{21} & \rho_{22} \end{pmatrix} = \frac{1}{2} \begin{pmatrix} 1 + s_3 & s_1 + i s_2 \\ s_1 - i s_2 & 1 - s_3 \end{pmatrix} = \frac{1}{2} (\hat{I}_2 + \mathbf{s} \cdot \boldsymbol{\sigma}), \quad (\text{A25})$$

where the vector $\mathbf{s} = \{s_1, s_2, s_3\}$ is known as the Bloch vector. For a pure state $\hat{\rho} = |\Psi\rangle\langle\Psi|$, the Bloch vector has unit length, $\sum_i |s_i|^2 = 1$, and points in some direction specified by the spherical coordinate angles θ and ϕ in a three-dimensional Euclidean space. The associated quantum state can be represented in terms of these angles as

$$|\Psi\rangle = \cos\left(\frac{\theta}{2}\right) e^{-i\phi/2} |\uparrow\rangle + \sin\left(\frac{\theta}{2}\right) e^{i\phi/2} |\downarrow\rangle. \quad (\text{A26})$$

Fig. A.1. Representation of the density matrix of a two-state system in terms of the Bloch sphere and Bloch vector. The three components of the Bloch vector $\mathbf{s} = \{s_1, s_2, s_3\}$ specify the density operator according to the parameterization of Eq. (A25). The two eigenvalues are $(1 \pm |\mathbf{s}|)/2$ and the two eigenvectors are specified by \mathbf{u} and $-\mathbf{u}$.



In general, and including the case of mixed states where $|\mathbf{s}| \leq 1$, the density operator of the form of Eq. (A25) has two eigenvalues

$$\begin{aligned} g_1 &= \frac{1}{2} \left[1 + \sqrt{s_1^2 + s_2^2 + s_3^2} \right] = \frac{1}{2} [1 + |\mathbf{s}|], \\ g_2 &= \frac{1}{2} \left[1 - \sqrt{s_1^2 + s_2^2 + s_3^2} \right] = \frac{1}{2} [1 - |\mathbf{s}|], \end{aligned} \tag{A27}$$

and its eigenvectors are determined by the two vectors \mathbf{u} and $-\mathbf{u}$ shown in the Bloch sphere in Fig. A.1. For pure states, where $|\mathbf{s}| = 1$, \mathbf{u} coincides with \mathbf{s} and its tip lies on the surface of the Bloch sphere. For a mixed state where $|\mathbf{s}| < 1$, vector \mathbf{u} points in the same direction as \mathbf{s} but unlike \mathbf{s} maintains unit length so that its tip always lies on the surface of the Bloch sphere. Equation (A26) can be used to express \mathbf{u} and $-\mathbf{u}$ in terms of the vectors in state space.

A.3 Entangled states

Let us now consider a two-particle (or two-mode) system (known also as a bipartite system) and, for simplicity, let us assume that each particle can be in either of two one-particle states $|\psi_1\rangle$ or $|\psi_2\rangle$. Using the notation

$|\psi_1^{(1)}\rangle$, particle 1 in state 1,

$|\psi_2^{(1)}\rangle$, particle 1 in state 2,

$|\psi_1^{(2)}\rangle$, particle 2 in state 1,

$|\psi_2^{(2)}\rangle$, particle 2 in state 2,

we consider a pure two-particle superposition state (in general an entangled state)

$$|\Psi\rangle = C_1 |\psi_1^{(1)}\rangle \otimes |\psi_2^{(2)}\rangle + C_2 |\psi_2^{(1)}\rangle \otimes |\psi_1^{(2)}\rangle \quad (\text{A28})$$

and clear from context throughout this book.) Clearly, this can be extended for multiparticle (multipartite) systems. For such multipartite systems, we can define reduced density operators for each of the subsystems by tracing the density operator over the states of all the other systems. In the present case, with the density operator of the two-particle system given by $\hat{\rho} = |\Psi\rangle\langle\Psi|$, the reduced density operator for particle 1 is

$$\begin{aligned}\hat{\rho}^{(1)} &= \text{Tr}_2 \hat{\rho} = \left\langle \psi_1^{(2)} \middle| \hat{\rho} \middle| \psi_1^{(2)} \right\rangle + \left\langle \psi_2^{(2)} \middle| \hat{\rho} \middle| \psi_2^{(2)} \right\rangle \\ &= |C_1|^2 \left| \psi_1^{(1)} \right\rangle \left\langle \psi_1^{(1)} \right| + |C_2|^2 \left| \psi_2^{(1)} \right\rangle \left\langle \psi_2^{(1)} \right|.\end{aligned}\quad (\text{A29})$$

This has the form for a mixed state for particle 1 as long as $C_i \neq 0$, $i = 1, 2$. Similarly, for particle 2,

$$\hat{\rho}^{(2)} = \text{Tr}_1 \hat{\rho} = |C_1|^2 \left| \psi_1^{(2)} \right\rangle \left\langle \psi_1^{(2)} \right| + |C_2|^2 \left| \psi_2^{(2)} \right\rangle \left\langle \psi_2^{(2)} \right|. \quad (\text{A30})$$

Evidently, when one of the particles is considered without regard to the other, it is generally in a mixed state. Thus one may characterize the degree of entanglement according to the degree of purity of either of the subsystems. If $\text{Tr}[\hat{\rho}^{(2)}]^2 = 1$, the state $|\Psi\rangle$ is not an entangled state; but if $\text{Tr}[\hat{\rho}^{(2)}]^2 < 1$ we may conclude that $|\Psi\rangle$ describes an entanglement between subsystems 1 and 2.

6.2 Quantum mechanics of beam splitters

At this point we must pause and consider the beam splitter in a fully quantum-mechanical context. In the previous chapter, we used the notion of a beam splitter in a somewhat cavalier manner. We were able to get away with it because, for “classical”-like light beams, coherent and thermal beams, the quantum and classical treatments of beam splitters agree. But at the level of a single or few photons, the classical approach to beam splitting produces erroneous and quite misleading results.

To see how classical reasoning over beam splitting goes wrong, let us consider first a classical light field of complex amplitude \mathcal{E}_1 incident upon a lossless beam splitter as indicated in Fig. 6.3. \mathcal{E}_2 and \mathcal{E}_3 are the amplitudes of the reflected and transmitted beams respectively. If r and t are the (complex) reflectance and transmittance respectively of the beam splitter, then it follows that

$$\mathcal{E}_2 = r\mathcal{E}_1 \quad \text{and} \quad \mathcal{E}_3 = t\mathcal{E}_1. \quad (6.1)$$

For a 50:50 beam splitter we would have $|r| = |t| = 1/\sqrt{2}$. However, for the sake of generality, we do not impose this condition here. Since the beam splitter is assumed lossless, the intensity of the input beam should equal the sum of the intensities of the two output beams:

$$|\mathcal{E}_1|^2 = |\mathcal{E}_2|^2 + |\mathcal{E}_3|^2 \quad (6.2)$$

BS

(Wrong!)

which requires that

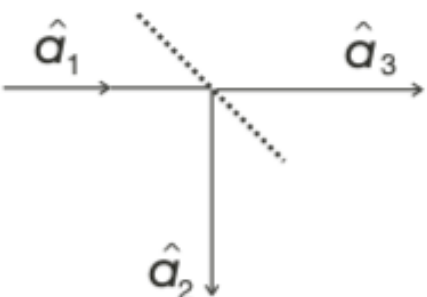


Fig. 6.4. Naïve, and incorrect, quantum mechanical depiction of a beam splitter.

$$|r|^2 + |t|^2 = 1. \quad (6.3)$$

To treat the beam splitter quantum mechanically we might try replacing the classical complex field amplitudes \mathcal{E}_i by a set of annihilation operators \hat{a}_i ($i = 1, 2, 3$) as indicated in Fig. 6.4. In analogy with the classical case we might try setting

$$\hat{a}_2 = r\hat{a}_1 \quad \text{and} \quad \hat{a}_3 = t\hat{a}_1. \quad (6.4)$$

However, the operators of each of the fields are supposed to satisfy the commutation relations

$$\left[\hat{a}_i, \hat{a}_j^\dagger \right] = \delta_{ij}, \quad [\hat{a}_i, \hat{a}_j] = 0 = \left[\hat{a}_i^\dagger, \hat{a}_j^\dagger \right] \quad (i, j = 1, 2, 3), \quad (6.5)$$

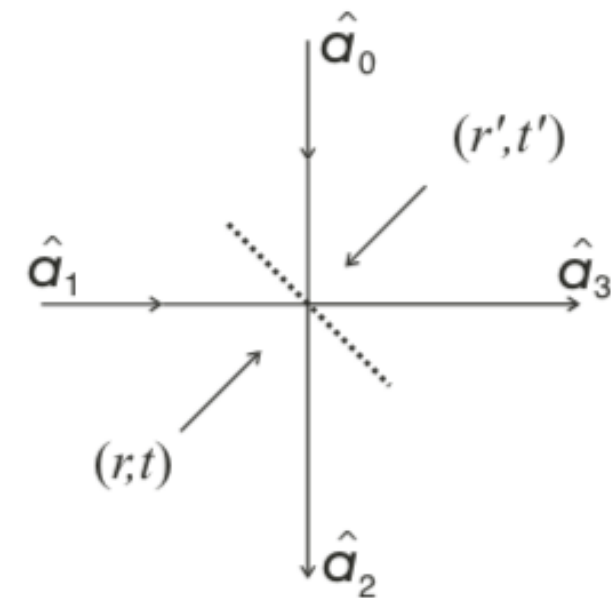
but it is easy to see that for the operators of Eq. (6.4) we obtain

$$\begin{aligned} \left[\hat{a}_2, \hat{a}_2^\dagger \right] &= |r|^2 \left[\hat{a}_1, \hat{a}_1^\dagger \right] = |r|^2, \\ \left[\hat{a}_3, \hat{a}_3^\dagger \right] &= |t|^2 \left[\hat{a}_1, \hat{a}_1^\dagger \right] = |t|^2, \\ \left[\hat{a}_2, \hat{a}_3^\dagger \right] &= rt^* \neq 0, \text{ etc.} \end{aligned} \quad (6.6)$$

Thus the transformations in Eq. (6.4) do not preserve the commutation relations and therefore cannot provide the correct quantum description of a beam splitter.

This conundrum is resolved as follows: in the classical picture of the beam splitter there is an unused “port” which, being empty of an input field, has no effect on the output beams. However, in the quantum-mechanical picture, the “unused” port still contains a quantized field mode albeit in the vacuum state and, as we have repeatedly seen, the fluctuations of the vacuum lead to important physical effects. The situation with the beam splitter is no exception. In Fig. 6.5 we indicate all the modes required for a proper quantum description of the beam splitter, \hat{a}_0 representing the field operator of the classically vacant input mode. Also indicated are two sets of transmittances and reflectances, allowing for the possibility of an asymmetric beam splitter. We now write the beam-splitter transformations for the field operators as

(Right!)



$$\hat{a}_2 = r\hat{a}_1 + t'\hat{a}_0, \quad \hat{a}_3 = t\hat{a}_1 + r'\hat{a}_0 \quad (6.7)$$

or collectively as

$$\begin{pmatrix} \hat{a}_2 \\ \hat{a}_3 \end{pmatrix} = \begin{pmatrix} t' & r \\ r' & t \end{pmatrix} \begin{pmatrix} \hat{a}_0 \\ \hat{a}_1 \end{pmatrix}. \quad (6.8)$$

It is easily seen that the commutation relations of Eq. (6.5) are satisfied as long as the following relations hold:

$$|r'| = |r|, |t| = |t'|, |r|^2 + |t|^2 = 1, r^*t' + r't^* = 0, \text{ and } r^*t + r't'^* = 0. \quad (6.9)$$

These relations are known as the reciprocity relations and can also be derived on the basis of energy conservation.

Fig. 6.5. The correct quantum-mechanical depiction of a beam splitter.

Let us examine a couple of relevant examples. The phase shifts of the reflected and transmitted beams depend on the construction of the beam splitter [4]. If the beam splitter is constructed as a single dielectric layer, the reflected and transmitted beams will differ in phase by a factor of $\exp(\pm i\pi/2) = \pm i$. For a 50:50 beam splitter, assuming the reflected beam suffers a $\pi/2$ phase shift, the input and output modes are related according to

$$\hat{a}_2 = \frac{1}{\sqrt{2}} (\hat{a}_0 + i\hat{a}_1), \quad \hat{a}_3 = \frac{1}{\sqrt{2}} (i\hat{a}_0 + \hat{a}_1). \quad (6.10)$$

Since the transformation between input and output modes must be unitary, we may write Eq. (6.8) as

$$\begin{pmatrix} \hat{a}_2 \\ \hat{a}_3 \end{pmatrix} = \hat{U}^\dagger \begin{pmatrix} \hat{a}_0 \\ \hat{a}_1 \end{pmatrix} \hat{U} \quad (6.11)$$

where \hat{U} is a unitary operator. This transformation constitutes a Heisenberg picture formulation of a beam splitter. For the specific transformation represented by Eq. (6.10), the operator \hat{U} has the form

$$\hat{U} = \exp \left[i \frac{\pi}{4} (\hat{a}_0^\dagger \hat{a}_1 + \hat{a}_0 \hat{a}_1^\dagger) \right], \quad (6.12)$$

easily checked using the Baker–Hausdorff lemma in Eq. (6.11).

As an example, consider the single photon input state $|0\rangle_0|1\rangle_1$ which we may write as $\hat{a}_1^\dagger|0\rangle_0|0\rangle_1$. For the beam splitter described by Eq. (6.10) we find that $\hat{a}_1^\dagger = (i \hat{a}_2^\dagger + \hat{a}_3^\dagger)/\sqrt{2}$. Thus we may write, using that $|0\rangle_0|0\rangle_1 \xrightarrow{\text{BS}} |0\rangle_2|0\rangle_3$,

$$\begin{aligned} |0\rangle_0|1\rangle_1 &\xrightarrow{\text{BS}} \frac{1}{\sqrt{2}} \left(i \hat{a}_2^\dagger + \hat{a}_3^\dagger \right) |0\rangle_2|0\rangle_3 \\ &= \frac{1}{\sqrt{2}} (i|1\rangle_2|0\rangle_3 + |0\rangle_2|1\rangle_3). \end{aligned} \quad (6.13)$$

This is an important result. It says that a single-photon incident at one of the input ports of the beam splitter, the other port containing only the vacuum, will be either transmitted or reflected with equal probability. Of course, this is precisely as we earlier claimed and explains why no coincident counts are to be expected with photon counters placed at the outputs of the beam splitter, as confirmed by the experiment of Grangier *et al.* [3]. Actually, because the beam splitter is well understood, the lack of coincident counts in the above experiment may be taken as an indication that the source is truly producing single-photon states. (Obviously,

One other point needs to be made about the output state of Eq. (6.13). It is an *entangled* state: it cannot be written as a simple product of states of the individual modes 2 and 3. The density operator (see Appendix A) for the (pure) state of Eq. (6.13) is

$$\begin{aligned}\hat{\rho}_{23} = & \frac{1}{2} \{ |1\rangle_2 |0\rangle_{32} \langle 1|_3 \langle 0| + |0\rangle_2 |1\rangle_{32} \langle 0|_3 \langle 1| \\ & + i |1\rangle_2 |0\rangle_{32} \langle 0|_3 \langle 1| - i |0\rangle_2 |1\rangle_{32} \langle 1|_3 \langle 0| \}.\end{aligned}\quad (6.14)$$

In placing detectors in the two output beams, we are measuring the full “coherence” as described by the state vector of Eq. (6.13) or equivalently the density operator of Eq. (6.14). Suppose, on the other hand, we make no measurement of, say, mode 3. Mode 2 is then described by the reduced density operator obtained by tracing over the states of the unmeasured mode (see Appendix A):

$$\begin{aligned}\hat{\rho}_2 = \text{Tr}_3 \hat{\rho}_{23} &= \sum_{n=0}^{\infty} {}_3 \langle n | \hat{\rho}_{23} | n \rangle_3 \\ &= \frac{1}{2} (|0\rangle_{22} \langle 0| + |1\rangle_{22} \langle 1|).\end{aligned}\quad (6.15)$$

This represents merely a statistical mixture, there being no “off-diagonal” coherence terms of the form $|0\rangle\langle 1|$ or $|1\rangle\langle 0|$. Thus placing a detector in only one of the output beams yields random results, 0 or 1, each 50% of the time, just as we would expect.

Before moving on to single-photon interference, let us consider two more examples of beam splitting. First we consider a coherent state, a classical-like state, rather the opposite of the highly nonclassical single-photon state, incident on the beam splitter with, again, only the vacuum in the other input port. That is, the initial state is $|0\rangle_0|\alpha\rangle_1 = \hat{D}_1(\alpha)|0\rangle_0|0\rangle_1$ where $\hat{D}_1(\alpha) = \exp(\alpha\hat{a}_1^\dagger - \alpha^*\hat{a}_1)$ is the displacement operator for mode 1. We may then, following the procedure above, obtain the output state according to

$$\begin{aligned}
 |0\rangle_0|\alpha\rangle_1 &\xrightarrow{\text{BS}} \exp\left[\frac{\alpha}{\sqrt{2}}(i\hat{a}_2^\dagger + \hat{a}_3^\dagger) - \frac{\alpha^*}{\sqrt{2}}(-i\hat{a}_2 + \hat{a}_3)\right]|0\rangle_2|0\rangle_3 \\
 &= \exp\left[\left(\frac{i\alpha}{\sqrt{2}}\right)\hat{a}_2^\dagger - \left(\frac{-i\alpha^*}{\sqrt{2}}\right)\hat{a}_2\right]\exp\left[\left(\frac{\alpha}{\sqrt{2}}\right)\hat{a}_3^\dagger - \left(\frac{\alpha^*}{\sqrt{2}}\right)\hat{a}_3\right]|0\rangle_2|0\rangle_3 \\
 &= \left|\frac{i\alpha}{\sqrt{2}}\right\rangle_2 \left|\frac{\alpha}{\sqrt{2}}\right\rangle_3. \tag{6.16}
 \end{aligned}$$

Evidently we obtain the result expected for a classical light wave where the incident intensity is evenly divided between the two output beams, e.g. half the incident average photon number, $|\alpha|^2/2$, emerges in each beam. We also naturally obtain the phase shift $i = e^{i\pi/2}$ for the reflected wave, as expected. Finally, note that the output is not entangled.

As a last example with operator transformations, we return to the strictly quantum domain and consider the situation where single photons are simultaneously injected into the two input ports of our 50:50 beam splitter, the incident state being $|1\rangle_0|1\rangle_1 = \hat{a}_0^\dagger\hat{a}_1^\dagger|0\rangle_0|0\rangle_1$. Again, following the previous procedure with $\hat{a}_0^\dagger = (\hat{a}_2^\dagger + i\hat{a}_3^\dagger)/\sqrt{2}$ and $\hat{a}_1^\dagger = (i\hat{a}_2^\dagger + \hat{a}_3^\dagger)/\sqrt{2}$ we have

$$\begin{aligned}
 |1\rangle_0|1\rangle_1 &\xrightarrow{\text{BS}} \frac{1}{2} \left(\hat{a}_2^\dagger + i\hat{a}_3^\dagger \right) \left(i\hat{a}_2^\dagger + \hat{a}_3^\dagger \right) |0\rangle_2|0\rangle_3 \\
 &= \frac{i}{2} \left(\hat{a}_2^\dagger\hat{a}_2^\dagger + \hat{a}_3^\dagger\hat{a}_3^\dagger \right) |0\rangle_2|0\rangle_3 \\
 &= \frac{i}{\sqrt{2}} (|2\rangle_2|0\rangle_3 + |0\rangle_2|2\rangle_3). \tag{6.17}
 \end{aligned}$$

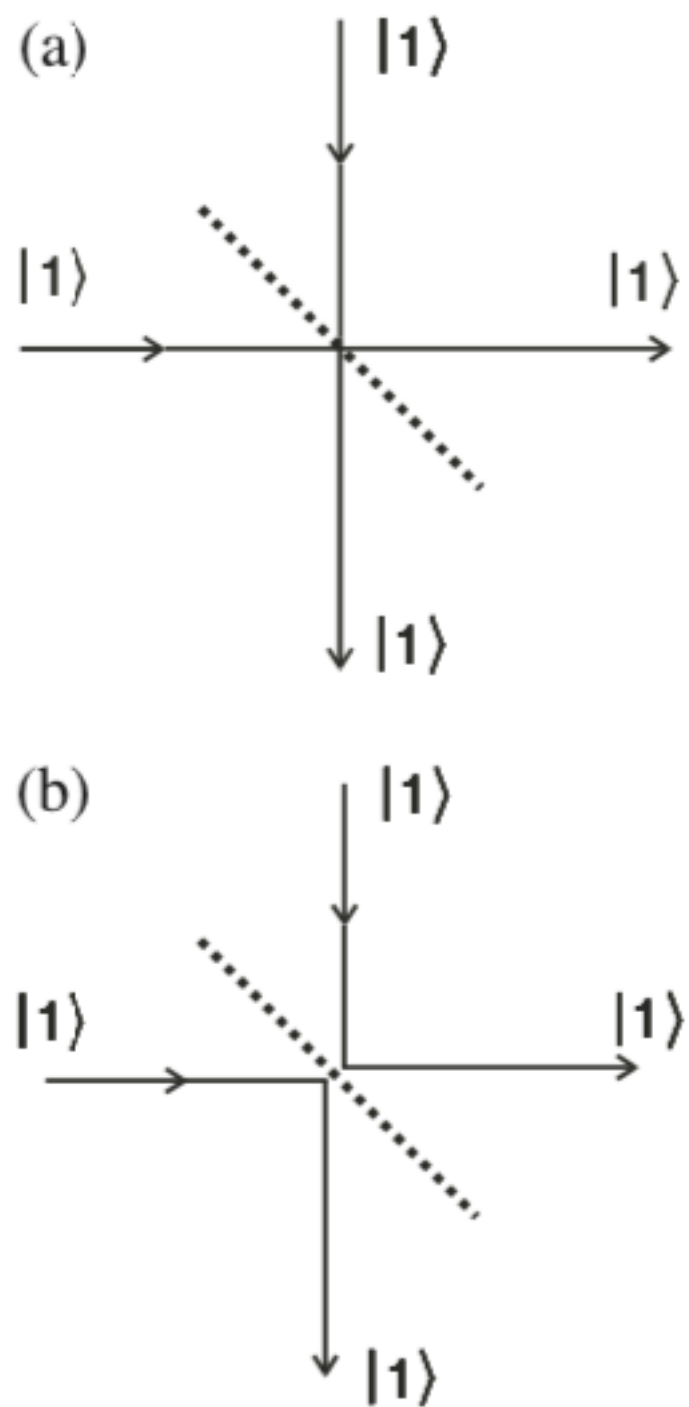


Fig. 6.6. Two indistinguishable processes with simultaneous single photon inputs. (a) Both photons are transmitted. (b) Both photons are reflected. These processes interfere destructively with each other.

Apparently, the two photons emerge together such that photo-detectors placed in the output beams should not register simultaneous counts. But unlike the case of a single incident photon, the physical basis for obtaining no simultaneous counts is not a result of the particle-like nature of photons. Rather, it is caused by interference (a wave-like effect) between two possible ways of obtaining the (absent) output state $|1\rangle_2|1\rangle_3$: the process where both photons are transmitted (Fig. 6.6(a)) and the process where they are both reflected (Fig. 6.6(b)). Note the indistinguishability of the two processes for the output state $|1\rangle_2|1\rangle_3$. There is a simple and rather intuitive way of understanding this result. Recall Feynman's rule [5] for obtaining the probability for an outcome that can occur by several indistinguishable processes: one simply adds the probability *amplitudes* of all the processes and then calculates the square of the modulus. Assuming that our beam splitter is described by Eq. (6.10), the reflected photons each acquire an $e^{i\pi/2} = i$ phase shift. The amplitude for transmission for each photon is $A_T = 1/\sqrt{2}$ and the amplitude for reflection for each is $A_R = i/\sqrt{2}$. The amplitude that *both* photons are transmitted is $A_T \cdot A_T$ and that both are reflected is $A_R \cdot A_R$. Thus the probability of the photons emerging in both output beams is

$$P_{11} = |A_T \cdot A_T + A_R \cdot A_R|^2 = \left| \frac{1}{\sqrt{2}} \cdot \frac{1}{\sqrt{2}} + \frac{i}{\sqrt{2}} \frac{i}{\sqrt{2}} \right|^2 = 0. \quad (6.18)$$

An experimental demonstration of this effect was first performed by Hong, Ou, and Mandel [6] and is discussed in Chapter 9.

9.2 The Hong–Ou–Mandel interferometer

In Chapter 6 we discussed what happens when twin single-photon states are simultaneously incident at each input port of a 50:50 beam splitter: the photons

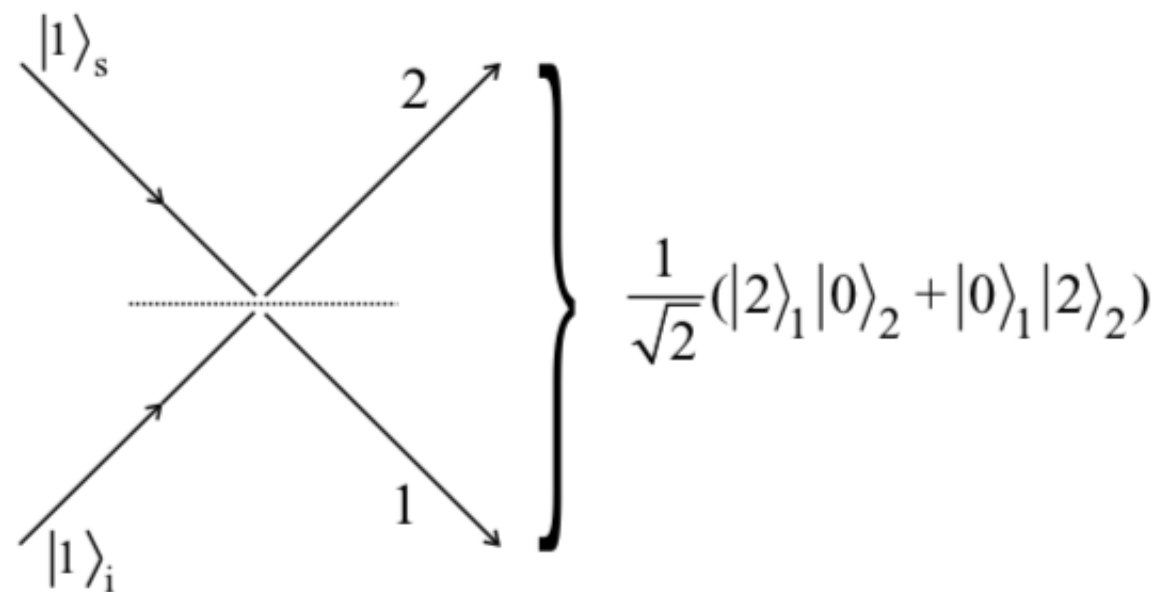


Fig. 9.5. Labeling of the output modes of a 50:50 beam splitter with inputs from the signal and idler beams of a type I down-converter. If single-photon states simultaneously fall onto the beam splitter, the output does not contain the term $|1\rangle_1|1\rangle_2$, for reasons discussed in Chapter 6.

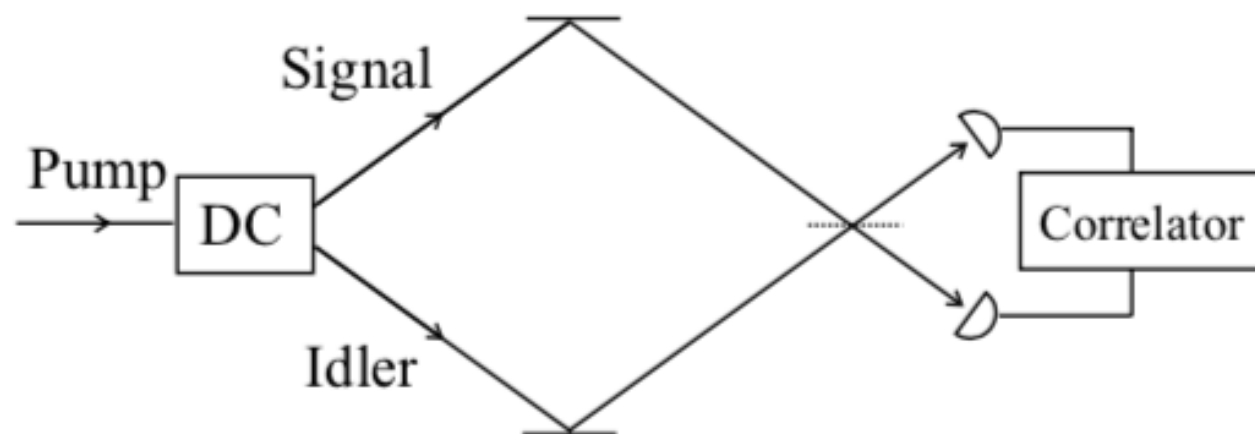
emerge together in one output beam or the other; no single photons ever emerge in both beams. Recall that for the input state $|1\rangle_s|1\rangle_i$ one has after the beam splitter the state

$$|\psi_{\text{BS}}\rangle = \frac{1}{\sqrt{2}}(|2\rangle_1|0\rangle_2 + |0\rangle_1|2\rangle_2), \quad (9.15)$$

where we have labeled the output modes 1 and 2 in accordance with Fig. 9.5.

fact, one could take the lack of simultaneous counts as an indication that the photons are incident on the beam splitter simultaneously. The first demonstration of this effect was by Hong, Ou and Mandel (HOM) in a now-classic experiment performed in 1987 [6]. In fact, the experiment was designed to measure the time separation between the two photons striking a beam splitter. A sketch of their experiment is given in Fig. 9.6. The nonlinear crystal is pumped to produce, assuming type I down-conversion, twin single-photon states whose beams are then directed to the input ports of a 50:50 beam splitter. Photon detectors are placed at the outputs of the beam splitter and the count signals are fed into a correlator. Changing the position of the beam splitter causes a slight time delay between the times the photons fall onto the beam splitter. With a slight nonzero time delay, the photons independently reflect or transmit through the beam splitter causing both detectors sometimes to fire within a short time of each other. It can be shown [6] that the rate of coincident detections, R_{coin} , has the form

$$R_{\text{coin}} \sim \left[1 - e^{-(\Delta\omega)^2(\tau_s - \tau_i)^2} \right], \quad (9.16)$$



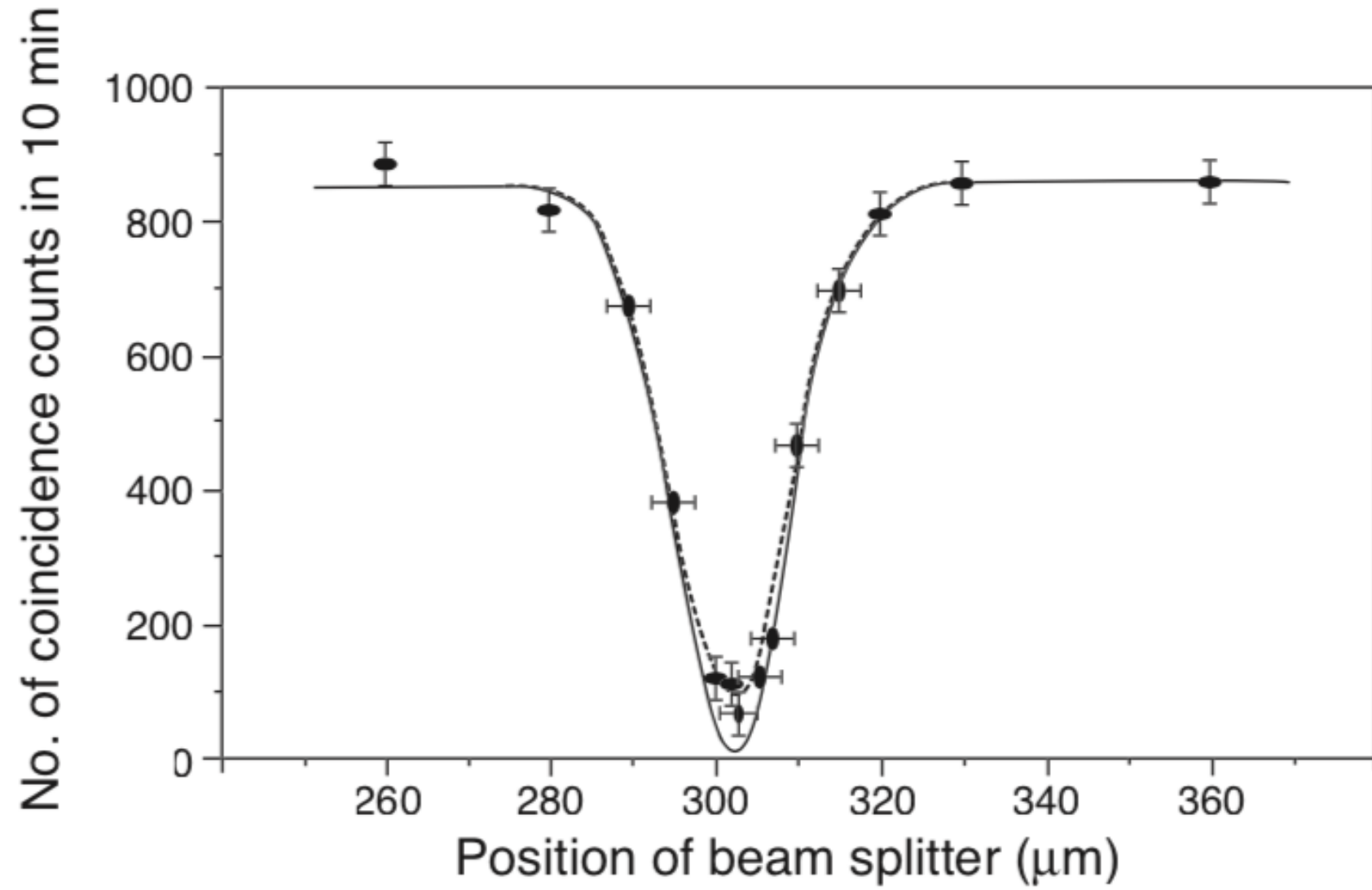


Fig. 9.7. Redrawn from the Hong–Ou–Mandel paper, the number of coincident counts in a 10 minute time interval as a function of the position of the beam splitter. The count rate does not go to zero exactly, owing to the fact that the beams do not perfectly overlap at the beam splitter. (Reprinted with permission.)

where $\Delta\omega$ is the bandwidth of the light and $c\tau_s$ and $c\tau_i$ are the distances that the signal and idler photons respectively travel from the down-converter to the beam splitter. The band width $\Delta\omega$ incorporates the reality that the signal and idler beams are not monochromatic, and its appearance in Eq. (9.16) results from the assumption that the spectral distribution is Gaussian. Obviously, for $\tau_s - \tau_i = 0$ we have $R_{\text{coin}} = 0$. The rate of coincidence counts rises to a maximum for $|\tau_s - \tau_i| \gg \tau_{\text{corr}}$, where $\tau_{\text{corr}} = 1/\Delta\omega$ is the correlation time of the photons.

The correlation time is of the order of a few nanoseconds, which is hard to measure with conventional techniques as detectors commonly used do not often have short enough resolving times. But this correlation time can be measured with the HOM interferometer. The experimental results are plotted in Fig. 9.7, reprinted from Reference [6]. Plotted here is the number of counts over an interval of 10 min against the position of the beam splitter (essentially the time separation) with the solid line representing the theoretical prediction. The experimental data do not go exactly to the predicted minimum because it is not possible for the beams precisely to overlap at the beam splitter. From the distribution of the counts, the correlation time of the two photons can be determined to be ~ 100 fs.